Article

Condensation Heat Transfer of R-407C in Helical Coiled Tube Heat Exchanger

Hamad Mohammad AlHajeri, Abdulrahman Almutairi, Mohamad Hamad Al-Hajeri *, Abdulrahman Alenezi[ID], Rashed ALajmi and Aboelyazeid Mohamed Koluib

Mechanical Power and Refrigeration Department, College of Technological Studies, Public Authority for Applied Education and Training, Shuwaikh 700030, Kuwait; hm.alhajeri@paaet.edu.kw (H.M.A.); asa.almutairi@PAAET.EDU.KW (A.A.); Ah.alenezi@paaet.edu.kw (A.A.); rm.alajmi@paaet.edu.kw (R.A.); am.koluib@paaet.edu.kw (A.M.K.)

* Correspondence: mh.alhajeri@paaet.edu.kw

check for updates

Abstract: The results of an experimental study to evaluate the characteristics of R-407C thermofluid during condensation in a helically coiled copper tube heat exchanger are presented. The effects of saturation temperature (T_{sat}), and mass and heat fluxes of refrigerant R-407C on thermal performance and pressure drop were determined. The relationship between the refrigerant wall subcooling and heat transfer coefficients was also investigated. This paper reports the effect of the temperature of the water used as cooling medium on the heat transfer rate of condensing R-407C. The study was conducted with mass flux of R-407C in the range of 100–450 kg/m^{2}s, mass flux of the coolant water in the range of 500–5000 kg/m^{2}s and T_{sat} of 31 °C, 35 °C, and 39 °C. Compared with a straight smooth tube, the use of the helical coiled (helicoidal) tube increased the condensation rate with a corresponding pressure drop that depended on the value of T_{sat} of the refrigerant and temperature of the coolant.

Keywords: heat transfer; condensation; R-407C; helical tube

1. Introduction

R-22 is a non-fully halogenated refrigerant that is commonly found in residential refrigeration units and air conditioning (A/C) systems. However, environmental concerns are driving the replacement of R-22 with R-407C or other suitable refrigerants. Fortunately, the vapor pressure of R-407C is the same as that of R-22, so it can be installed in existing systems with no major modifications. R-407C is a zeotropic mixed refrigerant that contains three hydrofluorocarbons (HFCs): difluoromethane (R-32), pentafluoroethane (R-125), and tetrafluoroethane (R-134a) in the proportions by weight of 23%, 25%, and 52%, respectively [1]. Due to the zeotropic nature of the refrigerant R-407C, a 6 °C temperature glide occurs through any heat transfer process [2]. This normally increases the thermal efficiency of refrigeration equipment.

The performance of R-407C was investigated experimentally by Devotta et al. [3] under retrofit conditions to replace the original R-22 in window A/C systems. The results of their study showed a lower cooling capacity, lower coefficient of performance, lower pressure drop, higher power consumption, and higher discharge pressures. Aprea and Greco [2], Wei et al. [4], and Jabaraj et al. [5] reported that R-407C is similar to R-22 with regard to the energy efficiency, temperature of the compressor discharge, pressure, and other performance parameters. Passos et al. [6] evaluated the overall heat transfer performance for R-407C and R-22 using a test rig with a horizontal, flat micro-fin tube condenser. They determined that the overall heat transfer coefficient (HTC) using R-407C was lower than that of R-22. Imran et al. [7] and Khalifa et al. [8] investigated numerically an air cooled condenser with

finned tube using R-22 and R-407C. They concluded that the performance of the two refrigerants was comparable.

Various tube configurations, such as pipes with added micro-fins, pipes of varying diameters, and pipes with helical grooves, have been installed in A/C systems to enhance their performance by increasing heat transfer rates. Several authors [9–11] have reported experimental investigations of the effects of the shapes of fins and sizes of pipes on pressure loss and heat transferred by condensation when using R-407C. Cavallini et al. [12] investigated the performance of R-22 and R-407C in micro-finned and smooth tubes, and showed that the addition of micro-fins increased the HTC for similar operating conditions. They found that the HTCs were lower for R-407C than for R-22 but the difference between the respective HTCs decreased with increase in mass flux.

HTCs and corresponding pressure drops in tubes with small diameters carrying R22, R-134a, R-407C and R-410A, have been studied by Wang et al. [13]. The condensation HTCs have been measured by Eckels and Tesene [14] for several refrigerants in smooth plain and enhanced pipes. Both studies found that the measured HTCs of R-22, R-134a, and R-410A were not significantly different given the uncertainty of the data. Local heat transfer in smooth horizontal pipes during condensation of R-407C and R-404A has been studied by Boissieux et al. [15].

The HTCs of condensation for the three refrigerants R-22, R-407C, and R-410A, for horizontal plain, low-fin, and turbo-C tubes were studied experimentally by Jung et al. [1], who measured the condensation HTCs for the three refrigerants with wall subcooling ranging from 3 °C to 8 °C. They also found the HTCs of refrigerant R-407C to be 24–75% lower for R-22 for the plain and low-fin tube but only 4–5% lower for the turbo-C tube.

Aroonrat and Wongwises [16–18] and Aroonrat et al. [17] performed experimental investigations on the condensation and evaporation of R-134a in dimpled helically coiled and dimpled horizontal tubes with different depths of dimpling. The dimples were to enhance the heat transfer by increasing the flow turbulence. The main observations were that, with respect to smooth tubes, dimpling of the horizontal tube could increase the HTC rate by up to 70% while dimpling of the helical tube increased the HTC by as much as 88%. Tang et al. [19] experimentally studied the effect on the condensation process of dimpling the outer surface of the inner tube of a co-axial tube-within-a-tube heat exchanger. They demonstrated that condensation was enhanced by approximately 178% for a dimpled inner tube compared to a smooth tube.

Yousef et al. [20] analyzed the comparative performance of the four refrigerants: R-22, R-134a, R-407C, and R-410A, as alternative cooling fluids in a condenser in a steam power plant. Vijayan and Srinivasan [21] experimentally investigated the performance of R-22 and R-407C in a window A/C system that was originally charged with R-22 but later charged with R-407C. They found that the coefficient of performance increased, and the power requirement and pressure ratio of the compressor were reduced.

Bohdal et al. [22] reported an experimental and analytical study into the pressure drop, heat transfer and condensation of three refrigerants R404A, R407C, and R410A flowing through vertical mini- and micro-channels at high-pressure.

Sieres et al. [23] experimentally investigated optimizing the performance of a R-407C domestic heat pump. The results of this study showed that for liquid-to-water systems the operating mode determines the optimum charge, and that the refrigerant charge has a linear relationship with the refrigerant level in the condenser.

Experimental and numerical investigations were carried out by Wang et al. [24] to assess the relative thermal performance of trilobal twisted helical coils with different cross-sectional areas. The thermal performance of the trilobal twisted tube was up to 1.31 times higher than that of plain and elliptical tubes. Solanki and Kumar [25–27] reported experimental studies of the condensation characteristic in helical coiled heat exchangers. The results revealed that as the quality of the vapor fell so did the pressure drop, which resulted in performance factor reduction. A thorough numerical analysis of the pitch, angle, and coil dimensions carried out on helical tube-in-tube and semicircular

heat exchangers was reported by Abu-Hamdeh et al. [28]. They concluded that the coefficient of performance for coils that were semi-circular in cross-section rather than circular was three times greater than for conventional tube-in-tube arrangements.

Mozafari et al. [29] experimentally investigated the effect of different inclination angles of helical coiled heat exchangers and found that deceasing the angle of inclination led to an increase in performance factor. Qiu et al. [30] conducted a numerical study on the effect of the inclination angle on R290 condensation in a mini-channel by evaluating the refrigerant charge, flow, and heat transfer. The results demonstrated that as the angle of inclination increased both HTC and pressure drop due to frictional forces also increased. Lee et al. [31] performed a numerical study of mini-tube heat exchangers by evaluating film condensation based on thermofluid characteristics. They highlighted that shear stresses over the film surface lead to an increased pressure drop and HTC. The liquid film formed on the wall during the condensation processes caused an increase in velocity.

Some A/C, chilled water systems, and heat pumps use R-407C as the working medium. R-407C and R-22 have very similar operating pressures and performance in dry expansion A/C arrangements. However, conventional systems that operate with R-407C are approximately 25–30% less efficient than systems that use R-22, especially at high ambient temperatures, which is very important in countries such as Kuwait. The size of a condenser could be increased to increase its efficiency. This would be feasible from the perspectives of installation, maintenance, and performance of a system if a helical tube were used; it would also improve the HTCs and require less space. Studies of other refrigerants, such as R-134a, have reported promising findings for the pressure drop and condensation heat transfer in helical pipes. However, to the best of our knowledge, no prior investigations have been conducted regarding the use of the R-407C refrigerant in a helical coiled tube heat exchanger.

In this investigation, local HTCs of R-407C during condensation were measured and recorded for systematic changes in the values of T_{sat}, coolant temperature, and refrigerant and coolant mass fluxes. How the subcooling temperature impacted on heat transfer performance at the higher value of T_{sat} of 39 °C in a helical coiled tube was evaluated. The study concentrated on the characteristics of the condensation component of the HTC associated with R-407C in the helicoidal tube.

2. Description of Experimental Test Rig

Figure 1 shows the experimental apparatus built to investigate pressure loss and condensation heat transfer for R-407C. The status of the saturated liquid after the reservoir was observed through a small glass window. A flow meter at the entrance to the evaporator was used to measure the R-407C flow rate. The basic arrangement contained a test section, three independent closed cycles, and a data logger. The three cycles are the cooling water, refrigerant, and hot water. The annular helical tube was copper, and its dimensions are shown in Figure 2.

The experimental apparatus was allowed to reach equilibrium by turning the vacuum pump on for an initial 4 h to make sure that all the refrigerant was evacuated from the loop, and the hot water and cold water loops were filled. This was followed by the injection of R-407C into the refrigerant loop. The temperature of the hot water loop mass flow was set to a suitable value to evaporate the refrigerant in the evaporator. Simultaneously, the cold water loop was set to a value to suitably cool the refrigerant in the condenser heat exchanger. The refrigerant was pumped to the evaporator then it was heated sufficiently to ensure it fully vaporized. After passing over the auxiliary electric heater, the vapor entered the helical tube condenser, where the cold water cooled the refrigerant. Following the helical tube condenser, the refrigerant was cooled to its approximate initial temperature using an air-cooled booster condenser.

Four sight glasses were installed throughout the test section to check the status of the refrigerant.

The helical tube test section was made of double tube copper of coil length 3 m. This was vertically mounted as presented in Figure 2. The inner tube was the refrigerant side and the outer tube was the waterside. The internal and external diameters of the inner tube were 7.39 mm and 9.54 mm, respectively. The coil section was 216 mm in diameter and 25.6 mm pitch and contained nine turns

with a total heat transfer area of 0.18 m². The helical tube heat exchanger was counter-flow where the water flowed upward and the refrigerant downward.
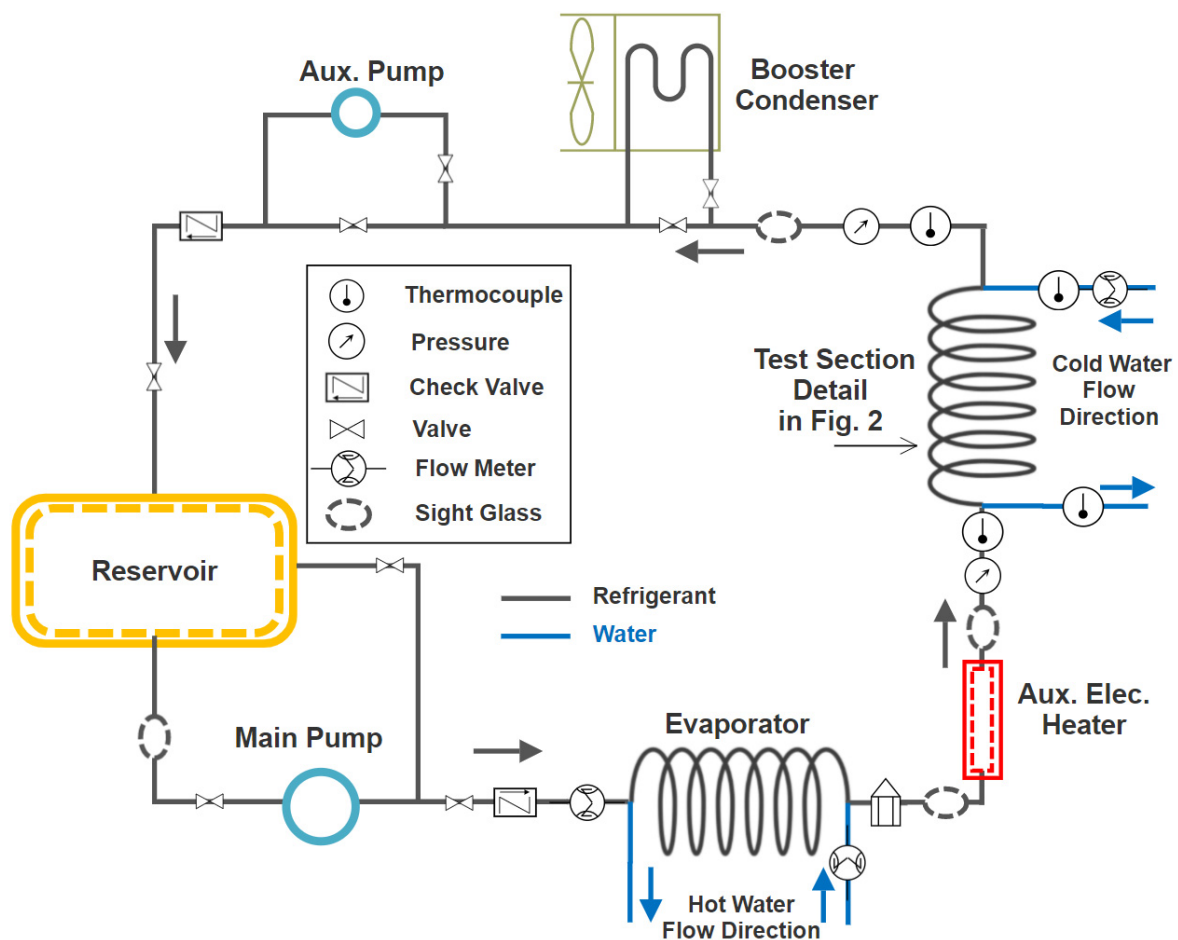
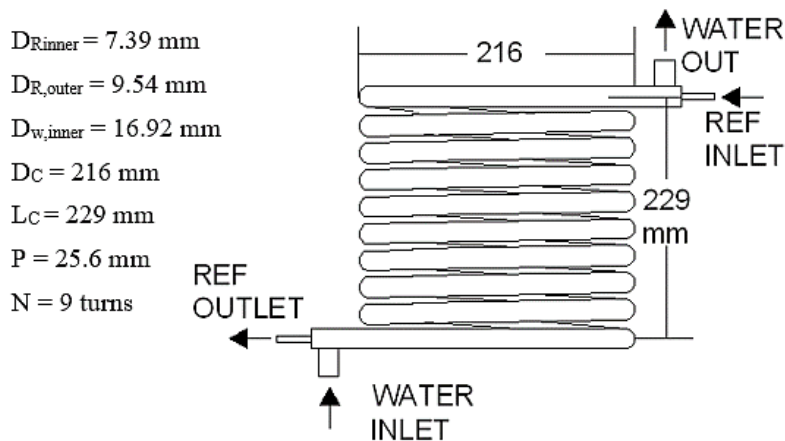**Figure 1.** Schematic diagram of experimental test system.

$D_{Rinner} = 7.39$ mm

$D_{R,outer} = 9.54$ mm

$D_{w,inner} = 16.92$ mm

$D_C = 216$ mm

$L_C = 229$ mm

$P = 25.6$ mm

$N = 9$ turns

Figure 2. Dimensions of test section.

3. Operation and Procedure

The inner tube carried a flow of saturated vapor of refrigerant R-407C. As the vapor lost heat to the coolant (chilled water) it condensed to a saturated liquid. The refrigerant entered the tank in the refrigerant cycle and flowed to the steam generator.

A bypass was included on the pump side of the cycle, to regulate the flow through the pipe into the tank. The refrigerant temperature was regulated by an electrical heater installed at the inlet to the condenser test section. The flow patterns at test section inlet and outlet were each observed by sight glasses. The temperature and pressure were measured at the points labelled T and P, respectively, for each of the refrigerant, hot water, and cooling water cycles.

The accuracy of the pressure measurement was ±0.1 psi. The entrance and exit temperatures of the R-407C and water were obtained using k-type thermocouples. The accuracy of the thermocouples was ±0.5 °C. Figure 1 shows the positions of the temperature sensors, and the readings were recorded by the data logger and retained for future use. The meters used to measure the flow rates of hot and cold water and R-407C were pulse turbine digital flow meters with an accuracy of ±0.002 L/min. The rig was filled with R-407C to the design pressure. All thermocouples were tested and adjusted to the operational range (0–150 °C). The flow meter and pressure gauge were also calibrated. The commercial data logger system, WebDAQ/100, was used to collect the required data.

4. Data Analysis

The data were analyzed to estimate the condensation HTCs and pressure losses in the helical tube. An energy balance was used to calculate the quality of the refrigerant vapor at the inlet to the condenser, according to the temperature of the water side of the helical tube condenser.

The heat transfer rate (Q) released from the refrigerant is defined as:

$$Q = m_w \, Cp_w \, (T_{w,o} - T_{w,i}) \tag{1}$$

where $T_{w,i}$ and $T_{w,o}$ are the cooling water temperatures inlet and outlet, respectively, Cp_w is the specific heat of water, and m_w is the mass flow rate of water [32].

The overall HTC can be expressed as:

$$Q = U_o \, A \, \Delta T_{LMTD} \tag{2}$$

where ΔT_{LMTD} is the logarithmic mean temperature difference for the two fluids used, U_o is the overall HTC, and A is the cross-sectional area. The overall HTC is calculated using Equation (3), derived from Equations (1) and (2):

$$U = \frac{m_w \, C_{Pw} \, (T_{w,o} - T_{w,i})}{A \, \Delta T_{LMTD}} \tag{3}$$

The influence of single-phase heat transfer in the helical pipe can be ignored. Therefore, the ΔT_{LMTD} is defined by:

$$\Delta T_{LMTD} = \frac{(T_{R,O} - T_{W,i}) - (T_{R,i} - T_{W,o})}{\ln[(T_{R,O} - T_{W,i})/(T_{R,i} - T_{W,o})]} \tag{4}$$

where $T_{R,i}$ and $T_{R,o}$ are the temperatures of the refrigerant, R-407C, at the inlet and outlet, respectively. The thermal properties of the refrigerants were estimated using the mean value of T_{sat} and mean pressure in the condenser. The HTC for the refrigerant was estimated by:

$$H_r = \frac{1}{\left[\frac{1}{U_o} - \frac{1}{h_w} - R_r\right]} \tag{5}$$

where h_w is the heat transfer coefficient for the coolant (water) [33], and R_r is thermal resistance for R-407C. The average temperature should be compatible with the cooling water's thermophysical properties. The mass flux, m_r, and mean heat flux, q, of R-470 are given by:

$$m_r = \frac{V_R \, \rho_R}{\frac{\pi}{4}(d^2_{i,2})} \tag{6a}$$

$$q = Q/\pi \, d_{i2} \, L \tag{6b}$$

where $d_{i,2}$ is the inner diameter of the inner tube, L is the length of the helical pipe, and V_R and ρ_R are the volumetric flows rate and density respectively of R-407C.

5. Results and Discussion

Three values of T_{sat}, 31 °C, 35 °C, and 39 °C, were used in the experiment to study how temperature affected the performance of the condenser in an A/C unit containing R-407C. For helical tubes carrying R-407C, the heat transfer rate for the refrigerant depends on flow patterns, pitch, curvature, and void fraction. In this investigation, the helical tube had a fixed pitch and curvature. Experiments were conducted for three different temperatures of the coolant as it entered the condenser. To simplify the study, the wall temperature was maintained at 3 °C, 5 °C, and 7 °C by adjusting the temperature of the coolant for each test.

The HTCs for condensation on the refrigerant side as a function of wall subcooling (2–10 °C) for the three values of T_{sat}; 31 °C, 35 °C, and 39 °C are shown in Figure 3. Subcooling is defined as the cooling of a liquid refrigerant below the condensing temperature at constant pressure. The wall subcooling temperature is the temperature difference between the refrigerant condensation temperature and the refrigerant temperature at the outlet of the condenser. Increasing the T_{sat} decreased the HTC, so minimum HTC occurred for the highest value of T_{sat} (39 °C). In addition, the HTCs decreased as wall subcooling temperatures increased. As the subcooled temperature increased, the temperature difference between the water and refrigerant temperatures decreased causing the HTC to decrease. As a result of the low wall subcooling temperature increases, the refrigerant temperature becomes close to the water cooler temperature. Thus, a lower wall subcooling temperature should be used to improve the performance.
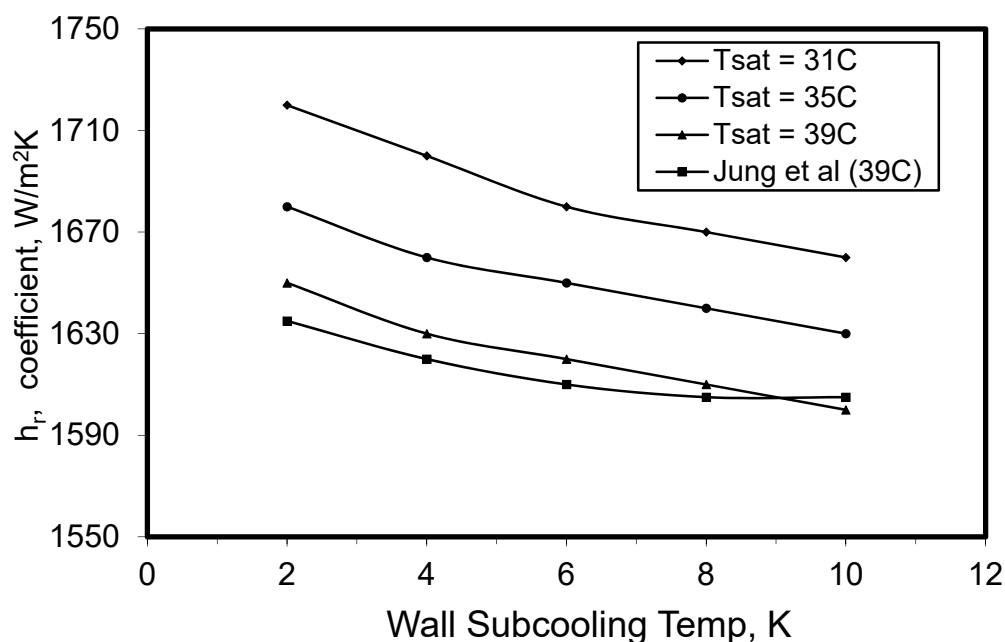

Figure 3. Condensation heat transfer coefficients of R-407C in helical tube as a function of wall subcooling, with comparative results from Jung et al. [11].

For similar values of T_{sat}, the HTC determined for a smooth tube was less than that obtained for a helicoidal tube. However, for a high wall subcooling temperature of approximately 10 °C, the HTC for the helical tube showed a slightly lower value compared to the coefficient for the smooth tube. In most practical applications the wall subcooling temperatures used are less than 9 °C, in which case the helical tube will have a higher HTC.

Figure 4 illustrates the overall HTC of R-407C in the helical tube against the subcooling temperature of the wall. For comparison, three values of T_{sat} were used: 31 °C, 35 °C, and 39 °C. The refrigerant overall HTCs reduced linearly as the wall subcooling temperature increased. Furthermore, these coefficients increased as the value of T_{sat} decreased. This occurred because of changes in the flow patterns and the reduction in heat transfer to the coolant. Furthermore, when the subcooling temperature increased, the thickness of the condensate layer increased, which decreased the overall HTC.
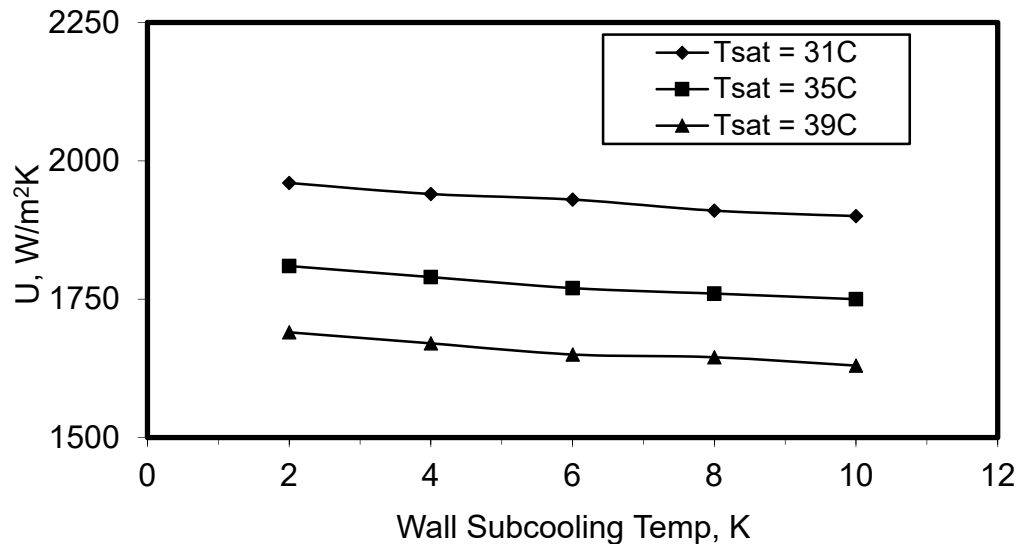

Figure 4. Overall heat transfer coefficient of R-407C in helical tube as a function of wall subcooling.

Pressure loss with wall subcooling temperature inside a helicoidal tube is shown in Figure 5. It was noticed that the pressure loss increased as the wall subcooling temperature increased. As the wall subcooling temperature increased, the refrigerant temperature decreased causing an increase in both density and viscosity generated friction. According to the fundamental laws of fluids, pressure loss has a positive relation with the density. For the three values of T_{sat} used, the pressure loss increased as T_{sat} decreased.
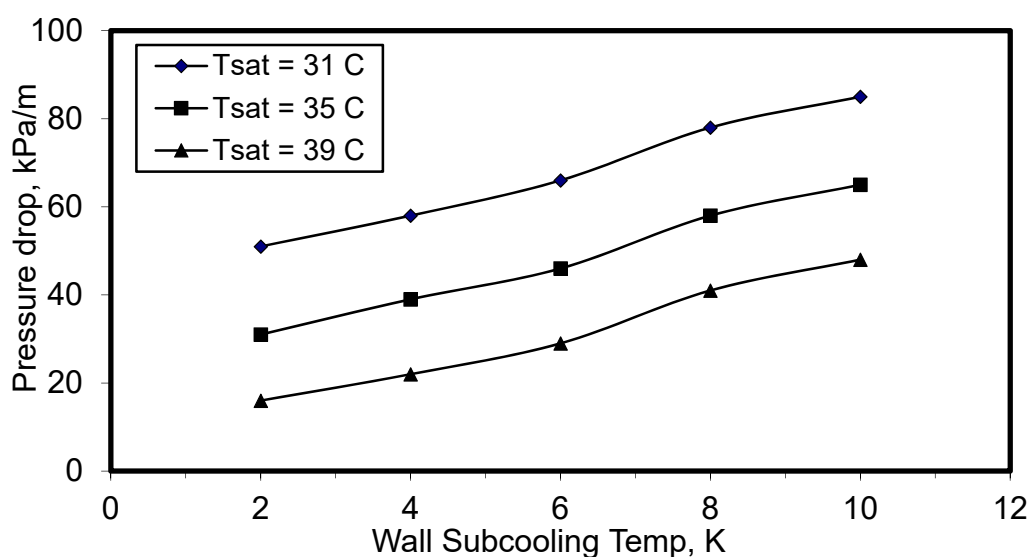

Figure 5. Pressure drop for R-407C in helical tube as a function of wall subcooling.

Massad et al. [34] compared the helical tube with other tube geometries and found that the loss in pressure was greater than for straight tubes, due to the greater complexity of the flow patterns in the

helical tube. For these different tube arrangements, the same mass flux in the helical tube will contain swirls and a higher turbulence intensity, which results in higher pressure loss.

Alhajeri et al. [35] compared the pressure drop in a helical tube using R-134a with the pressure drop in a micro-finned straight tube as reported by Eckels and Tesene [14]. It was concluded that the pressure losses in helicoidal tubes were greater than the loss in micro-finned straight tubes in the case of low refrigerant mass flux.

However, with decreasing refrigerant mass flux, the difference between the pressure losses in the helical tube and the micro-fin straight tube increased, particularly as the temperature of the cooling water increased. If they had used a greater range of mass flux in the study, the drop in pressure in the straight micro-fin tube would have become greater than the decrease in the helical tube because of the loss of pressure produced by the presence of the fins. In the case of a straight tube without fins, as is well known, the pressure loss increases proportional to the length.

For R-407C, Figure 6 shows the mean heat flux as a function of coolant water mass flux for the three temperatures 3 °C, 5 °C, and 7 °C. In this figure, two parameters were fixed: the mass flux of the refrigerant was maintained at 155 kg/m^{2}s and the value of T$_{sat}$ at 35 °C. The relation indicates that the heat flux of the refrigerant is considerably higher when the wall temperature is lower, and the rate at which the heat flux increases is higher at lower wall temperatures. This is because of the decreases in pressure, viscosity, and density of the refrigerants, which reduce friction, and this allows the refrigerant to have a higher velocity. For low values of the coolant mass flux, about 500 kg/m^{2}s, the heat fluxes converge to a value of about 5 kW/m^2. The heat flux increases with increase in coolant mass flux and decreases with increase in coolant temperature. Therefore, for enhanced performance it is recommended that a high coolant mass flux is used with low coolant temperature.
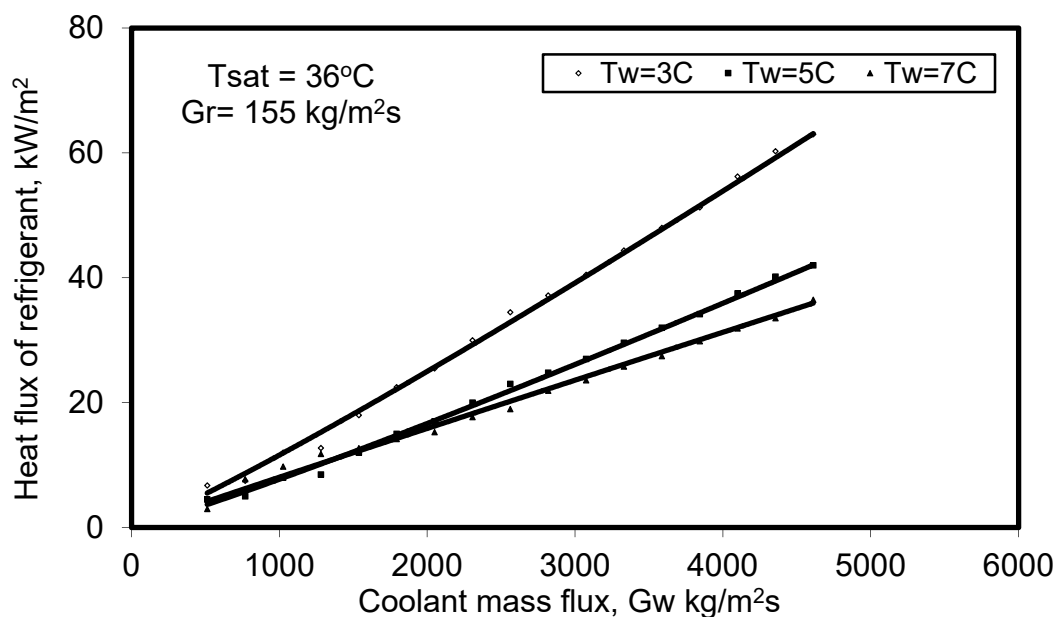

Figure 6. Average heat flux of refrigerant R-407C as a function of coolant (water) mass flux through heat exchanger for three coolant temperatures.

Figure 7 shows how coolant (water) mass flux varies with refrigerant mass flux with T$_{sat}$ constant at 35 °C. We see that for the three coolant water temperatures, 3 °C, 5 °C, and 7 °C, the refrigerant mass flux increases as the mass flux of the coolant water increases but decreases as the coolant water temperature increases. It follows that A/C systems that use R-407C require low coolant temperatures for optimal operation.
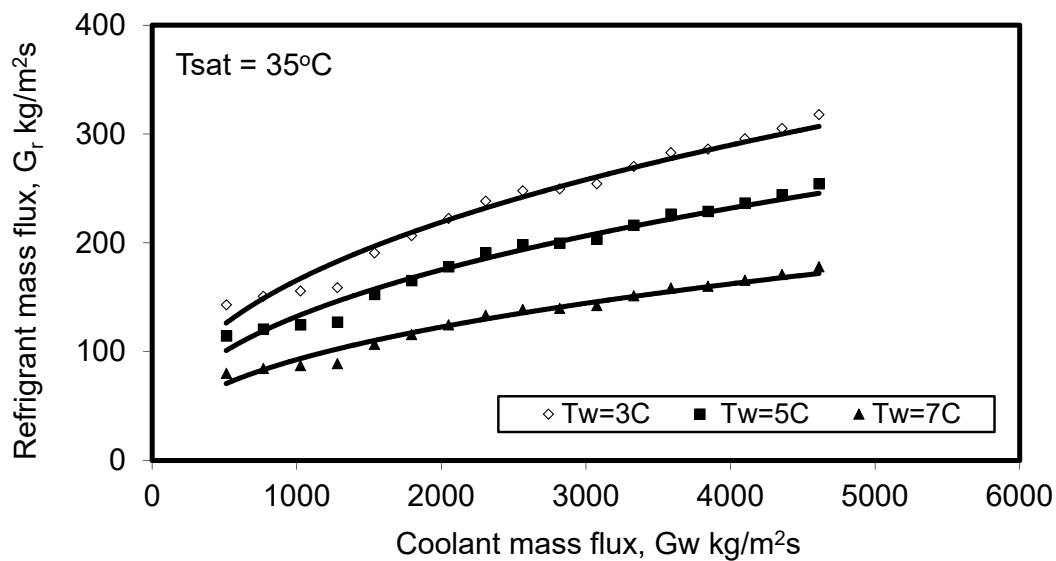
Figure 7. Mass flux of refrigerant R-407C as a function of coolant (water) mass flux through heat exchanger for three coolant temperatures.

Figure 8 shows the HTC for R-407 as a function of refrigerant mass flux for the three values of Tw: 3 °C, 5 °C, and 7 °C, when using the helical tube heat exchanger. As the refrigerant mass flux increases, the refrigerant HTC also increases. The mass flux in Equation (6) shows that the increase in the velocity of the refrigerant and liquid film causes the mass flux of the refrigerant to increase. This occurred concurrently with the growth of the centrifugal force in the helical pipe which acts on the inner wall increasing the turbulence within the flow of refrigerant and enhancing the heat transfer. Once again, we see that an increase in coolant water temperature reduces the heat transfer, so the use of coolant with a lower temperature increases the temperature difference and improves the refrigerant HTC. With condensation the greater the volume of vapor that condensed, the lower will be the vapor velocity, and the thicker the liquid film, both of which will reduce the average HTC.
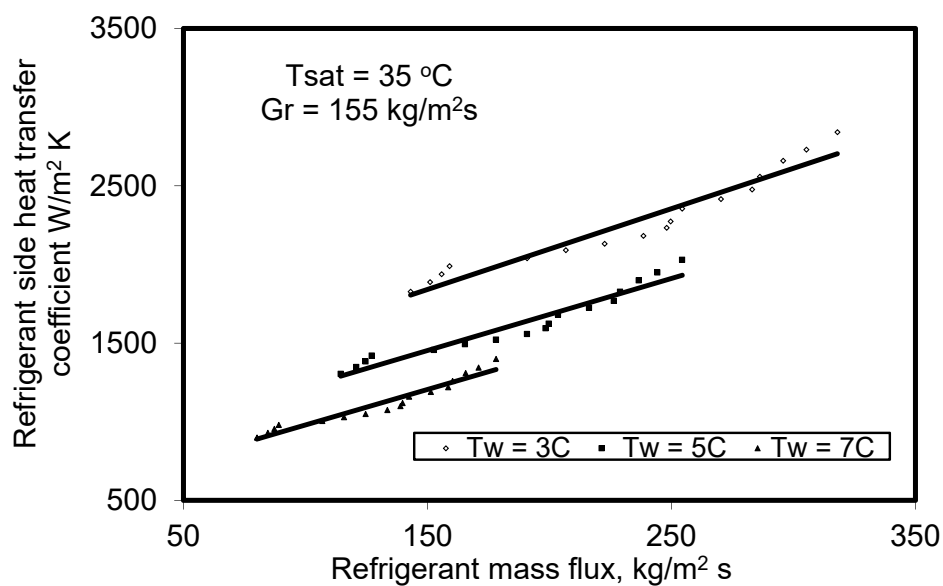

Figure 8. Effect of coolant (water) mass flux on refrigerant R-407C heat transfer coefficient.

The vapor quality of the R-407C refrigerant at condenser inlet and outlet, x_{in} and x_{out}, respectively, can be evaluated using Equation (7a,b).

$$x_{in} = \frac{h_{Ri} - h_{wi}}{h_{vi}} \tag{7a}$$

$$x_{out} = \frac{h_{Ro} - h_{wo}}{h_{vo}} \tag{7b}$$

where h_w is the enthalpy of the saturated liquid; h_v is the latent heat of vaporization, measured using the entrance and exit temperatures of the test section; h_R is the enthalpy of the refrigerant; and *i* and *o* are the entrance and outlet of the condenser.

The experimentally measured values of HTC for R-407C as a function of the vapor quality is shown in Figure 9 for T_{sat} values of 31 °C, 35 °C, and 39 °C. The vapor quality used in this figure is the arithmetic mean of inlet and outlet qualities. The average HTC increases with increase in vapor quality (lower liquid fraction). This is because the velocity of the refrigerant increased at higher values of vapor quality (more gas phase) at which the shear was increased. Furthermore, secondary flow, turbulence, and HTC were all increased owing to the continuous bend of the helical pipe. The void fraction of the mixture increased when the vapor quality increased, forming a thinner condensate film at the lower part of the pipe and increasing the interfacial area, which reduced the thermal resistance. Consequently, the heat transfer mechanism was more efficient. The HTCs were higher at lower values of T_{sat} and rose as vapor quality improved.
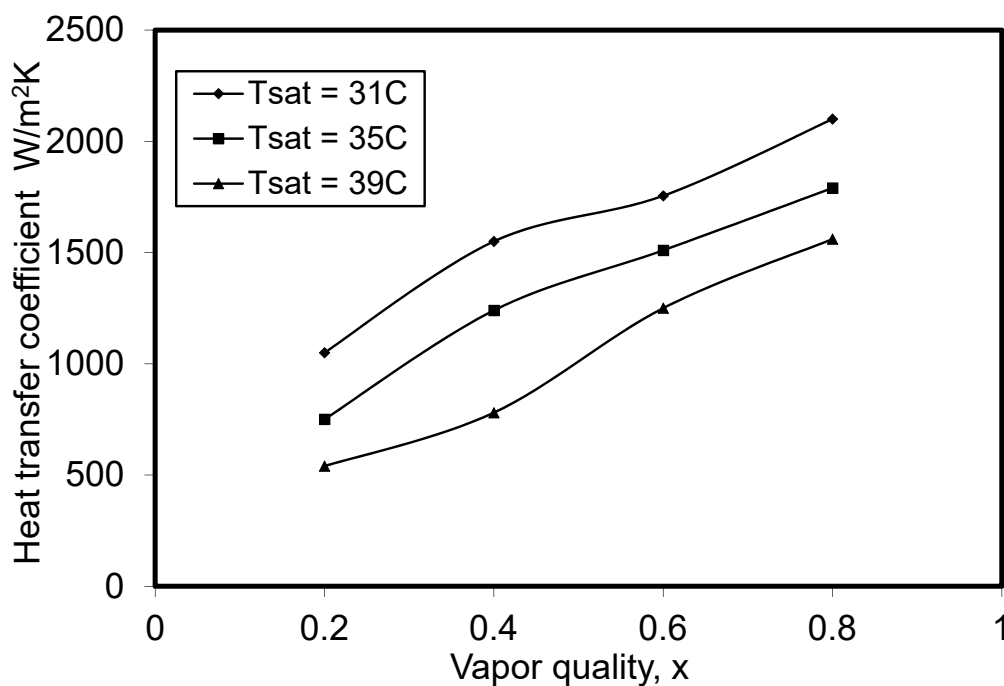

Figure 9. Heat transfer coefficient as a function of average vapor quality of refrigerant.

Uncertainties

The analysis of the uncertainties of the test section of the helical tube for the condensation HTCs was based on Moffat's work [36] which also considered the pressure, temperature, water and mass refrigerant flow rates. Referring to the experimental conditions that were used, the uncertainties that were associated with the refrigerant's mass flow rate, cooling water volume flow rate, cooling water Reynolds number, and temperature differences were 0.25%, 0.34%, 3%, and ±0.4 °C, respectively. In addition, uncertainties in the water side HTCs, refrigerant side HTCs, and overall HTCs were 7%, 21%, and approximately 18%, respectively.

6. Conclusions

The pressure loss and heat transfer coefficient for refrigerant R-407C flowing in a helicoidal copper pipe have been investigated experimentally utilizing a purpose-built test rig. Three saturation vapor temperatures of 31 °C, 35 °C, and 39 °C were used in the study with the temperature of the wall sub-cooling in the range 2–10 °C.

The experimental results showed that as the refrigerant mass flux increased, the heat transfer coefficient increased. As the temperature of the saturated vapor of the refrigerant decreased, both the refrigerant side HTC and the overall HTC increased. The refrigerant pressure loss in the helical tube was found to be dependent on coolant wall temperature and refrigerant, T_{sat}. It increased with increase in wall subcooling temperature and increased with decrease in T_{sat}. Thus, as the coolant (water) mass flux increased, the pressure loss in the helical tube decreased.

This investigation has provided information that could be applied to enhance the design of helical coiled tube condensers for A/C and refrigeration applications specially in hot ambient temperature: we recommend the use of a lower wall subcooling temperature, low coolant temperature, high mass flux of coolant, and high mass flux of refrigerant. In addition, using lower temperatures for the water coolant resulted in a higher HTC on the refrigerant side. Furthermore, for higher ambient temperature, a helical coiled tube performs better than a smooth tube through the high HTC to the same T_{sat}.

Conflicts of Interest: The authors declare no conflict of interest.

Nomenclature

A	heat transfer area, m^2
C_P	specific heat, kJ/kg K
D	diameter of the coil, m
d	diameter of the copper tube, m
H	heat transfer coefficient, W/m^2 K
L	total length of the helical pipe, m
m	mass flow rate, kg/s
N	number of turns in the coil
Gr	mass flux, kg/m^{2}s
P	pitch of helical coil, m
q	heat flux, W/m^2
Q	heat transfer rate
R	heat transfer resistance of the wall of the tube, m^2 K/W
T	temperature, K
U	overall heat transfer coefficient, W/m^2 K
x	vapor quality
ρ	density, kg/m^3
ΔT_{LMTD}	logarithmic mean temperature difference, K
i	inlet or inner
o	outlet, outer, overall
r	wall resistance
w	water
2	inner tube
1	outer tube

References

1. Jung, D.; Kim, C.-B.; Hwang, S.-M.; Kim, K.-K. Condensation heat transfer coefficients of R22, R407C, and R410A on a horizontal plain, low fin, and turbo-C tubes. *Int. J. Refrig.* **2003**, *26*, 485–491. [CrossRef]

2. Aprea, C.; Greco, A. Performance evaluation of R22 and R407C in a vapour compression plant with reciprocating compressor. *Appl. Therm. Eng.* **2003**, *23*, 215–227. [CrossRef]

3. Devotta, S.; Padalkar, A.; Sane, N. Performance assessment of HCFC-22 window air conditioner retrofitted with R-407C. *Appl. Therm. Eng.* **2005**, *25*, 2937–2949. [CrossRef]

4. Wei, C.; Lin, S.; Wang, C. System performance of a split-type unit having R-22 and R-407C as working fluids. In Proceedings of the American Society of Heating, Refrigerating and Air-Conditioning Engineers (ASHRAE) Winter Meeting, Philadelphia, PA, USA, 24–28 February 1997; p. 1136.

5. Jabaraj, D.; Avinash, P.; Lal, D.M.; Renganarayan, S. Experimental investigation of HFC407C/HC290/HC600a mixture in a window air conditioner. *Energy Convers. Manag.* **2006**, *47*, 2578–2590. [CrossRef]

6. Passos, J.C.; Kuser, V.F.; Haberschill, P.; Lallemand, M. Convective boiling of R-407c inside horizontal microfin and plain tubes. *Exp. Therm. Fluid Sci.* **2003**, *27*, 705–713. [CrossRef]

7. Imran, A.; Hatem, F.; Hadi, F. A Comparative Study of the Performance of Finned Tube Air Cooled Condenser with Refrigerants R22 and R407C. *Al-Nahrain J. Eng. Sci.* **2017**, *20*, 657–665.

8. Khalifa, A.H.N.; Fataj, J.J.; Shaker, A.K. Performance Study on a Window Type Air Conditioner Condenser Using Alternative Refrigerant R407C. *Eng. J.* **2017**, *21*, 235–243. [CrossRef]

9. Sami, S.; Desjardins, D. Heat transfer of ternary mixtures inside enhanced surface tubing. *Int. Commun. Heat Mass Transf.* **2000**, *27*, 855–864. [CrossRef]

10. Koyama, S.; Lee, S.-M. Condensation of a ternary zeotropic mixture in a horizontal microfin tube. *Therm. Sci. Eng.* **2001**, *9*, 1–7.

11. Jung, D.; Cho, Y.; Park, K. Flow condensation heat transfer coefficients of R22, R134a, R407C, and R410A inside plain and microfin tubes. *Int. J. Refrig.* **2004**, *27*, 25–32. [CrossRef]

12. Cavallini, A.; Censi, G.; Del Col, D.; Doretti, L.; Longo, G.A.; Rossetto, L.; Zilio, C. Experimental heat transfer coefficient and pressure drop during condensation of R22 and R407C inside a horizontal microfin tube. *Int. Heat Transf. Conf.* **2002**. [CrossRef]

13. Wang, C.-C.; Chiang, S.-K.; Chang, Y.-J.; Chung, T.-W. Two-Phase Flow Resistance of Refrigerants R-22, R-410A and R-407C in Small Diameter Tubes. *Chem. Eng. Res. Des.* **2001**, *79*, 553–560. [CrossRef]

14. Eckels, S.J.; Tesene, B.A. A comparison of R-22, R-134a, R-410a, and R-407c condensation performance in smooth and enhanced tubes: Part 1, Heat transfer. In Proceedings of the ASHRAE Annual Meeting, Seattle, WA, USA, 18–23 September 1999.

15. Boissieux, X.; Heikal, M.; Johns, R. Two-phase heat transfer coefficients of three HFC refrigerants inside a horizontal smooth tube, part I: Evaporation. *Int. J. Refrig.* **2000**, *23*, 269–283. [CrossRef]

16. Aroonrat, K.; Wongwises, S. Experimental investigation of condensation heat transfer and pressure drop of R-134a flowing inside dimpled tubes with different dimpled depths. *Int. J. Heat Mass Transf.* **2019**, *128*, 783–793. [CrossRef]

17. Aroonrat, K.; Ahn, H.S.; Jerng, D.-W.; Asirvatham, L.G.; Dalkılıç, A.S.; Mahian, O.; Wongwises, S. Experimental study on evaporative heat transfer and pressure drop of R-134a in a horizontal dimpled tube. *Int. J. Heat Mass Transf.* **2019**, *144*, 118688. [CrossRef]

18. Aroonrat, K.; Wongwises, S. Condensation heat transfer and pressure drop characteristics of R-134a flowing through dimpled tubes with different helical and dimpled pitches. *Int. J. Heat Mass Transf.* **2018**, *121*, 620–631. [CrossRef]

19. Tang, W.; Kukulka, D.J.; Li, W.; Simth, R. Comparison of the Evaporation and Condensation Heat Transfer Coefficients on the External Surface of Tubes in the Annulus of a Tube-in-Tube Heat Exchanger. *Energies* **2020**, *13*, 952. [CrossRef]

20. Yousef, K.; Assefa, A.; Hegazy, A.; Engeda, A. Comparative Study of Using R-410A, R-407C, R-22, and R-134a as Cooling Medium in the Condenser of a Steam Power Plant. *J. Eng. Gas Turbines Power* **2014**, *137*, 022002. [CrossRef]

21. Vijayan, R.; Srinivasan, P. Experimental evaluation of internal heat exchanger influence on R-22 window air conditioner retrofitted with R-407C. *Therm. Sci.* **2010**, *14*, 39–47. [CrossRef]

22. Bohdal, T.; Charun, H.; Kruzel, M.; Sikora, M. High pressure refrigerants condensation in vertical pipe minichannels. *Int. J. Heat Mass Transf.* **2019**, *134*, 1250–1260. [CrossRef]

23. Sieres, J.; Ortega, I.; Cerdeira, F.; Álvarez, E. Influence of the refrigerant charge in an R407C liquid-to-water heat pump for space heating and domestic hot water production. *Int. J. Refrig.* **2020**, *110*, 28–37. [CrossRef]

24. Wang, G.; Dbouk, T.; Wang, D.; Pei, Y.; Peng, X.; Yuan, H.; Xiang, S. Experimental and numerical investigation on hydraulic and thermal performance in the tube-side of helically coiled-twisted trilobal tube heat exchanger. *Int. J. Therm. Sci.* **2020**, *153*, 106328. [CrossRef]

25. Solanki, A.K.; Kumar, R. Condensation frictional pressure drop characteristic of R-600a inside the horizontal smooth and dimpled helical coiled tube in shell type heat exchanger. *Int. J. Therm. Sci.* **2020**, *154*, 106406. [CrossRef]

26. Solanki, A.K.; Kumar, R. Condensation of R-134a inside dimpled helically coiled tube-in-shell type heat exchanger. *Appl. Therm. Eng.* **2018**, *129*, 535–548. [CrossRef]

27. Solanki, A.K.; Kumar, R. Condensation of R-134a inside micro-fin helical coiled tube-in-shell type heat exchanger. *Exp. Therm. Fluid Sci.* **2018**, *93*, 344–355. [CrossRef]

28. Abu-Hamdeh, N.; Bantan, R.A.R.; Tlili, I. Analysis of the thermal and hydraulic performance of the sector-by-sector helically coiled tube heat exchangers as a new type of heat exchangers. *Int. J. Therm. Sci.* **2020**, *150*, 106229. [CrossRef]

29. Mozafari, M.; Behabadi, M.A.; Qobadi-Arfaee, H.; Fakoor-Pakdaman, M. Condensation and pressure drop characteristics of R600a in a helical tube-in-tube heat exchanger at different inclination angles. *Appl. Therm. Eng.* **2015**, *90*, 571–578. [CrossRef]

30. Qiu, G.; Li, M.; Cai, W. The effect of inclined angle on flow, heat transfer and refrigerant charge of R290 condensation in a minichannel. *Int. J. Heat Mass Transf.* **2020**, *154*, 119652. [CrossRef]

31. Lee, Y.-T.; Hong, S.; Chien, L.-H.; Lin, C.-J.; Yang, A.-S. Heat transfer and pressure drop of film condensation in a horizontal minitube for HFO1234yf refrigerant. *Appl. Energy* **2020**, *274*, 115183. [CrossRef]

32. Chang, C.-C.; Luo, W.-J.; Lu, C.-W.; Cheng, Y.-S.; Tsai, B.-Y.; Lin, Z.-H. Effects of process air conditions and switching cycle period on dehumidification performance of desiccant-coated heat exchangers. *Sci. Technol. Built Environ.* **2016**, *23*, 1–10. [CrossRef]

33. Kang, H.; Lin, C.-X.; Ebadian, M. Condensation of R134a flowing inside helicoidal pipe. *Int. J. Heat Mass Transf.* **2000**, *43*, 2553–2564. [CrossRef]

34. Mosaad, M.E.-S.; Al-Hajeri, M.; Al-Ajmi, R.; Koliub, A.M. Heat transfer and pressure drop of R-134a condensation in a coiled, double tube. *Heat Mass Transf.* **2009**, *45*, 1107–1115. [CrossRef]

35. Alhajeri, M.H.; Koluib, A.M.; Alajmi, R.; Kalim, S.P. Effect of Coolant Temperature on the Condensation Heat Transfer in Air-Conditioning and Refrigeration Applications. *Exp. Heat Transf.* **2009**, *22*, 58–72. [CrossRef]

36. Moffat, R.J. Describing the uncertainties in experimental results. *Exp. Therm. Fluid Sci.* **1988**, *1*, 3–17. [CrossRef]